



## Article

# Analytical Investigation of the Time-Dependent Stagnation Point Flow of a CNT Nanofluid over a Stretching Surface

Ali Rehman <sup>1</sup>, Anwar Saeed <sup>2,\*</sup>, Zabidin Salleh <sup>1</sup>, Rashid Jan <sup>3</sup> and Poom Kumam <sup>2,4,\*</sup>

<sup>1</sup> Department of Mathematics, Faculty of Ocean Engineering Technology and Informatics, Universiti Malaysia Terengganu, Kuala Nerus 21030, Terengganu, Malaysia; alirehmanhd8@gmail.com (A.R.); zabidin@umt.edu.my (Z.S.)

<sup>2</sup> Center of Excellence in Theoretical and Computational Science (TaCS-CoE), Science Laboratory Building, Faculty of Science, King Mongkut's University of Technology Thonburi (KMUTT), 126 Pracha-Uthit Road, Bang Mod, Thung Khru, Bangkok 10140, Thailand

<sup>3</sup> Department of Mathematics, University of Swabi, Swabi 94640, Pakistan; rashid\_ash2000@yahoo.com

<sup>4</sup> Department of Medical Research, China Medical University Hospital, China Medical University, Taichung 40402, Taiwan

\* Correspondence: anwarsaeed769@gmail.com (A.S.); poom.kum@kmutt.ac.th (P.K.)

**Abstract:** The heat transfer ratio has an important role in industry and the engineering sector; the heat transfer ratios of CNT nanofluids are high compared to other nanofluids. This paper examines the analytical investigation of the time-dependent stagnation point flow of a CNT nanofluid over a stretching surface. For the investigation of the various physical restrictions, single and multi-walled carbon nanotubes (SWCNTs, MWCNTs) were used and compared. The defined similarity transformation was used, to reduce the given nonlinear partial differential equations (PDEs) to nonlinear ordinary differential equations (ODEs). The model nonlinear ordinary differential equations were solved, with an approximate analytical (OHAM) optimal homotopy asymptotic method being used for the model problem. The impact of different parameters such as magnetic field parameter, unsteady parameter, dimensionless nanoparticles volume fraction, Prandtl number, and Eckert number are interpreted using graphs, in the form of the velocity and temperature profile.

**Keywords:** CNTs; nanofluid; stretching surface; heat transfer; stagnation point



**Citation:** Rehman, A.; Saeed, A.; Salleh, Z.; Jan, R.; Kumam, P. Analytical Investigation of the Time-Dependent Stagnation Point Flow of a CNT Nanofluid over a Stretching Surface. *Nanomaterials* **2022**, *12*, 1108. <https://doi.org/10.3390/nano12071108>

Academic Editors: M. M. Bhatti, Kambiz Vafai, Sara I. Abdelsalam and Yang-Tse Cheng

Received: 1 February 2022

Accepted: 21 March 2022

Published: 28 March 2022

**Publisher's Note:** MDPI stays neutral with regard to jurisdictional claims in published maps and institutional affiliations.



**Copyright:** © 2022 by the authors. Licensee MDPI, Basel, Switzerland. This article is an open access article distributed under the terms and conditions of the Creative Commons Attribution (CC BY) license (<https://creativecommons.org/licenses/by/4.0/>).

## 1. Introduction

The study of Magneto–Marangoni convection, which is caused by surface tension, has been a popular research topic for scientists and engineers in recent years. This is due to the numerous applications, including thin liquid layer scattering, atomic reactors, semiconductor processing, dynamic uses in the welding process, crystal development, material science, varnishes, silicon melting, and many more. In addition, the Marangoni phenomena are commonly exploited in fine art mechanisms, such as pigment on the ground. The colorant or dye is suspended on the outside surface of the needed medium, such as water or another thickness fluid, in this technique. To make a print, the medium is encased in rag or paper. Pop et al. [1] investigated the various characteristics of the Marangoni convection technique for thermo-solutal boundary films. Marangoni convection was researched by Al-Mudhaf and Chamkha [2], utilizing a temperature and solute gradient moving through a porous medium. Wang [3] used perturbation solutions to implement the Marangoni convection concept in a thin film spray. By examining the power-law model under Marangoni, Chen [4] extended Wang's idea. Magyari and Chamkha [5] used the flow assumption of a high Reynolds number to study the influence of Marangoni convection. Lin et al. [6,7] investigated the architectures of a MHD Marangoni-convective exchange of power-law nanoliquid with temperature gradients in a MHD Marangoni-convective exchange of power-law nanoliquid. Aly and Ebaid [8] used the Laplace transformation on a

permeable surface and convective boundary film conditions, to compute the exact solution of Marangoni flow of a viscid nanoliquid. Ellahi et al. [9] studied the effects of various forms of nanoscale materials in an ethylene glycol-based aqueous nanofluid solution. The analytical results of Marangoni convective heat convection of power-law liquids in permeable media were computed by Xu and Chen [10]. Sheikholeslami [11] proposed an ideal model of two-phase Marangoni convective MHD nanoliquid hydrothermal flow. Various types of research have recently focused on the Marangoni convection flow in various flow features [12–16].

The energy crisis has become a major topic in recent years, with many academics attempting to discover advanced resources for restoring energy and controlling the consumption of heat transfer devices. Solids, gases, and liquids are all part of these resources. The addition of tiny (1–100 nm) solid metal particles into common liquids can improve their thermal efficiency. Working liquids with low heat transfer rates, such as bioliquids, polymeric solutions, various oils, greases, water, toluene, refrigerants, ethylene glycol, and others, are widely utilized in a variety of engineering and scientific applications. The well-known metallic entities and their oxides,  $\text{TiO}_2$ ,  $\text{Al}_2\text{O}_3$ , are placed in operating liquids to improve the thermal efficiency of these liquids. Choi [17] established the optimal theory of nanoscale metallic object dispersal in molecular fluids from this perspective. He conducted an experiment on nanoliquids and came to the conclusion that the contribution of these metallic items is a fantastic means for improving thermal proficiency. After combining nanoparticles of Cu at a rate of 0.3 percent volume fraction, Eastman et al. [18] observed a 40% improvement in the thermal performance of  $\text{C}_2\text{H}_6\text{O}_2$ . Khamis et al. [19] investigated the heat transport of  $\text{Cu}_2\text{Al}_3 + \text{H}_2\text{O}$  and nanoliquids through a porous pipe. Using  $\text{Al}_2\text{O}_3$  water nanoliquids, Malvandi and Ganji [20] investigated the effect of nanoparticle volume fraction on heat transfer rate improvement. Using the  $\text{Al}_2\text{O}_3 + \text{H}_2\text{O}$  nanoliquid flow through an upright cone, Reddy and Chamkha [21] discovered a significant increase in the rate of heat exchange. The movement of  $\text{Al}_2\text{O}_3$ -based non-Newtonian nanoliquids over a circular region was studied by Barnoon and Toghraie [22]. A study of nanofluid flow in a microchannel was completed by Hossenine et al. [23]. Carbon nanotubes (CNTs) are carbon tube-shaped particles of nanometer dimensions. The strong connection between carbon atoms distinguishes CNTs, and the tubes can have a high aspect ratio. CNTs are classed as single-walled or multi-walled nanotubes (SWNTs or MWNTs), depending on their structure. Different properties of CNT nanoparticles, such as physical, electrical, optical, and thermal, have boosted the use of nanofluids in engineering processes such as nano- and microelectronics, biosensors, ultra-capacitors, atomic reactors, gas storage, textile engineering, flat-plate display, and medicinal tools.

Nonporous cleansers, solar collectors, and a variety of coatings are among the many other applications for CNTs. The flow of a nanoliquid containing nanoparticles was discussed by Xie and colleagues [24] (MWCNTs). The thermal characteristics of nanoliquids were improved using these nanoparticles. The motion and heat transport properties of CNT nanofluids over a tube were studied by Ding et al. [25]. Haq et al. [26] used a stretching plate to calculate the numerical results of three distinct molecular liquid flows incorporating CNT nanoparticles. When the volume fraction of particles was 15%, Ueki et al. [27] found that the improvement in thermal properties of carbon blocks increased by 7% and nanopowder increases by 19%. The 3D flow of both nanoparticles (SWCNTs/water and MWCNTs/water) and motor oil was studied by Rehman et al. [28]. The numerical research of CNT–nanoliquids flow and heat transport through a perpendicular cone was developed by Sreedevi et al. [29]. The flow of SWCNT- and MWCNT-nanofluid with a revolving and extending disc was studied by Jyothi et al. [30]. In this respect, a number of researchers [31,32] have recently looked at the flow of CNT nanoparticles from various physical perspectives. Due to their presence in a variety of technical and engineering applications, such as cylinder surface patterning [33], the cooling of optical fibers [34], greasing films on the inner walls of tubes, and condensing vapor on heat pipes [35] have been thoroughly investigated. Frenkel [36] pioneered modelling research on liquid film

flow on a cylinder surface. Different models have been investigated to analyze the falling of a liquid film on a perpendicular cylinder, including the thin liquid model [37] and the thick film model [38]. The experimental examination of thin fluid film motion on a vertical cylinder by Duprat et al. [39] revealed that four different forms of flow can occur in the scheme. The 3D flow of a thin liquid sheet on a vertical cylinder was studied by Ding and Wong [40]. Alshomrani and Gul [41] investigated a thin film spray of an  $\text{Al}_2\text{OCu}_3$  nanoliquid over a slick cylinder. Ali et al. [42] investigated the CNTs nanofluid across a stretched surface utilizing blood as a base fluid. The nonlinear dynamics of thin fluid flows through a hot cylinder were studied by Chao et al. [43].

Inspired by the literature, we present an analytical investigation of time-dependent stagnation point flow of a CNT nanofluid over a stretching surface. The key objective of this analysis was to improve the heat transfer ratio, because heat transfer ratio has some important applications in the engineering and industrial sectors. In our research paper, we used a CNT nanofluid, which has a higher heat transfer ratio compared to other nanofluids; we also discuss the convergence of the approximate analytical method and the effects of different parameters on fluid particle motion, as well as a comparison of the present research work with the previously published work. The flow analysis is considered over a stretching surface; the similarity transformation is used to convert the nondimensionless form of the differential equation to the dimensionless form. The following characteristics indicate the study's novelty: A uniform magnetic field was used to study the approximate analytical solution of the thin layer flow of a nanofluid. This was the first investigation of the analytic solution of this model. Liao et al. [44–46] found an approximate solution technique that does not depend upon the small parameters used to discover the problem's series solution. Using the BVP 2.0 program, the residual sum of the acquired results was calculated up to the 25th order approximation [47–51].

## 2. Mathematical Formulation

Consider the time-dependent 2D stagnation point flow of a CNT nanofluid along with heat transfer in the presence of a magnetic field on a stretching surface. The continuity, momentum, and temperature equation for the given flow problem is given below:

$$\frac{\partial u}{\partial x} + \frac{\partial v}{\partial y} = 0, \quad (1)$$

$$\rho_{nf} \left( \frac{\partial u}{\partial t} + u \frac{\partial u}{\partial x} + v \frac{\partial u}{\partial y} \right) = \left( U_s \frac{dU_s}{dx} + \mu_{nf} \frac{\partial^2 u}{\partial y^2} - \sigma_{nf} B_0^2 (u - U_s) \right), \quad (2)$$

$$\frac{\partial T}{\partial t} + u \frac{\partial T}{\partial x} + v \frac{\partial T}{\partial y} = \frac{k}{(\rho C_p)_{nf}} \frac{\partial^2 T}{\partial y^2} + \frac{\mu_{nf}}{(\rho C_p)_{nf}} \left( \frac{\partial u}{\partial y} \right)^2 \quad (3)$$

$T$  represents temperature of the surface,  $k$  represents the thermal conductivity,  $\rho$  represents the density of the fluid, and  $c_p$  represents the specific heat.  $u$  and  $v$  are the velocity component along the  $x$  and  $y$  directions, the distance along the sheet is denoted by  $x$  and the distance perpendicular to the sheet is denoted by  $y$ , the velocity of the stagnation point is denoted by  $U_w = ax$  with  $a > 0$ ,  $\nu$  represents kinematic viscosity of the fluid.

The boundary condition for velocity and temperature are

$$\begin{aligned} u &= U_w, v = 0 \text{ at } y = 0; u \rightarrow U_s \text{ as } y \rightarrow \infty, \\ T &= T_w \text{ at } y = 0; T \rightarrow T_\infty \text{ as } y \rightarrow \infty. \end{aligned} \quad (4)$$

$T_w$  represents the temperature of the sheet, and  $T_\infty$  represents free stream temperature. The stream functions for the given flow problem are

$$u = \frac{\partial \psi'}{\partial y} \text{ and } v = -\frac{\partial \psi'}{\partial x}. \quad (5)$$

Similarity transformations of the defined flow problem are

$$\psi = \sqrt{\frac{av_f}{1-\alpha t}} x f(\eta) \text{ And } \eta = y \sqrt{\frac{a}{v_f(1-\alpha t)}}, \theta(\eta) = \frac{T - T_\infty}{T_W - T_\infty}. \tag{6}$$

Putting Equations (5) and (6) into Equations (1)–(4), gives

$$f''' + (1-\phi)^{2.5} \left( (1-\phi) + \phi \frac{\rho_s}{\rho_f} \right) \left[ f f'' - f'^2 - S \left( f' + \frac{\eta}{2} f'' \right) \right] - (1-\phi)^{2.5} M f' = 0 \tag{7}$$

$$\frac{k_{nf}}{k_f} \theta'' - \left( (1-\phi) + \phi \frac{(\rho C_p)_{CNT}}{(\rho C_p)_f} \right) \left( \text{Pr}(\theta' f) + \frac{S}{2} \text{Ec}(\eta \theta') \right) = 0 \tag{8}$$

With boundary conditions

$$\begin{aligned} f(\eta) &= 0, f'(\eta) = \frac{c}{a} \text{ at } \eta = 0, f'(\eta) \rightarrow 1 \text{ as } \eta \rightarrow \infty, \\ \theta(\eta) &= 1 \text{ at } \eta = 0; \theta(\eta) \rightarrow 0 \text{ as } \eta \rightarrow \infty. \end{aligned} \tag{9}$$

$$\begin{aligned} \frac{\rho_{nf}}{\rho_f} &= (1-\phi) + \phi \left( \frac{\rho_{CNT}}{\rho_f} \right), \frac{\mu_{nf}}{\mu_f} = (1-\phi)^{-2.5}, \frac{(\rho C_p)_{nf}}{(\rho C_p)_f} = \left[ (1-\phi) + \phi \left( \frac{(\rho C_p)_{CNT}}{(\rho C_p)_f} \right) \right], \\ \frac{k_{nf}}{k_f} &= \frac{1-\phi + 2\phi \left( \frac{k_{CNT}}{k_{CNT}-k_f} \right) \ln \left( \frac{k_{CNT}+k_f}{2k_f} \right)}{1-\phi + 2\phi \left( \frac{k_f}{k_{CNT}-k_f} \right) \ln \left( \frac{k_{CNT}+k_f}{2k_f} \right)}. \end{aligned} \tag{10}$$

where prime denotes differentiation with respect to  $\eta$  and the constant  $a > 0, b > 0, \text{Pr} = \frac{\gamma}{\alpha}$  is the Prandtl number.  $\alpha$  is thermal diffusivity,  $\text{Ec} = \frac{u_w^2}{C_p(T_w - T_\infty)}$  represents the Eckert number,  $S = \frac{\gamma}{b}$ , represents the unsteady parameter,  $\phi$  represents a dimensionless nanoparticle volume fraction, and  $M = \frac{\sigma^* B_0^2}{\rho_f b}$  represents the magnetic field

*The Skin Friction and Nusselt Number*

In this analysis, the two key important quantities are skin friction and Nusselt number, given as

$$\text{Re}_x^{\frac{1}{2}} C_{xf} = - \frac{(1-\phi)^{-2.5}}{(1-\phi) + \phi \left( \frac{\rho_1}{\rho_f} \right)} f''(0), \text{Re}_x^{-\frac{1}{2}} Nu_x = - \frac{k_s}{k_{nf}} \theta'(0), \tag{11}$$

where  $\text{Re}_x = U_w L / \nu$ .

**3. Method of Solution**

We apply the basic idea of OHAM to the given problem given below.

$$f''' - f f'' - f'^2 - f'' - f' = 0, f(0) = 0, f'(\infty) = 1, f'(1) = \frac{c}{a} \tag{12}$$

where  $\eta$  is a similarity variable,  $f(\eta)$  is related to the stream function and prime denote derivative with respect to  $\eta$ . Let  $\lambda > 0$  denote a kind of spatial scale parameter by means of transformation

$$f(\eta) = \lambda^{-1} u(\xi), \xi = \lambda \eta \tag{13}$$

The original Equation (12) becomes

$$\begin{aligned} u'''(\xi) - u u''(\xi) - (u'(\xi))^2 - u''(\xi) - u'(\xi) &= 0 \\ u(0) = 0, u'(\infty) = 1, u(1) &= \frac{c}{a} \end{aligned} \tag{14}$$

The boundary condition  $u'(\infty) = 1$ , the asymptotic property  $u \rightarrow \zeta$  as  $\zeta \rightarrow \infty$ . According to the these information,  $u(\zeta)$  can be stated in the form

$$u(\zeta) = A_{0,0} + \zeta + \sum_{m=1}^{\infty} \sum_{n=0}^{\infty} A_{m,n} \zeta^n \exp(-m\zeta) \quad (15)$$

where  $A_{m,n}$  represent constants. The so called solution expression of  $u(\zeta)$  has an important role in OHAM. Subsequently, we have four boundary conditions, rendering to the solution (15) the simplest four terms of  $u(\zeta)$  are  $A_{0,0}, \zeta, A_{1,0} \exp(-\zeta), A_{2,0} \exp(-\zeta)$ , we chose the initial solution in the form of

$$u_0(\zeta) = A_{0,0} + \zeta + A_{1,0} \exp(-\zeta) + A_{2,0} \exp(-\zeta) \quad (16)$$

where  $A_{0,0}, A_{1,0}, A_{2,0}$  are unknown constants. Enforcing  $u_0(\zeta)$  to satisfy the three boundary conditions, we have  $A_{0,0} = 0, A_{1,0} = -1, A_{2,0} = 0$  so we have

$$u_0(\zeta) = \zeta - 1 + e^{-\zeta} \quad (17)$$

According to the solution (17), we should chose the linear operator  $L$ , in a manner that  $L(u) = 0$

$$L(C_0 + C_1\zeta + C_2e^{-\zeta}) \quad (18)$$

The estimation for velocity and for temperature are

$$f_0(\eta) = \frac{c}{a} + e^{-\eta} \quad (19)$$

$$\theta_0(\eta) = e^{-\eta} + 1 \quad (20)$$

which is obtained from the linear operator

$$L_f = f''' - ff'' = 0, L_\theta = \theta'' = 0, \quad (21)$$

#### 4. Results and Discussion

In this section, we discuss the influence of the different parameters, such as  $\{M, S, \phi, Pr, Ec\}$  (magnetic field parameter, unsteady parameter, dimensionless nanoparticles volume friction, Prandtl number and Eckert number) on both  $f'(\eta)$  and  $\theta(\eta)$ . The CNT nanofluid is used for the enhancement of heat improvement applications. The flow investigation has studied on a movable surface, along with the magnetic field. To transform the nonlinear partial differential equation (PDE) to a nonlinear ordinary differential equation (ODE), we used the defined similarity transformation. The nonlinear differential equations were solved with the help of the approximate analytical method, named the optimal homotopy asymptotic method (OHAM). The convergence control parameter for the particular problems is also discussed in table form. With the help of the analytical method, a solution of the nonlinear differential equations for velocity and temperature profiles were obtained. The results of the particular problem are emphasized in Figures 1–9; Figures 1–3 represent the effect of dissimilar parameters on velocity distribution, Figures 4 and 5 represent the effect of dissimilar parameters on temperature profile, Figures 6 and 7 represent the effect of dissimilar parameters on  $C_f$  (skin friction), and Figures 8 and 9 represent the effect of dissimilar parameters on the Nusselt number. From Figures 6 and 7 we can observe that skin friction is the function increasing the magnetic field parameter, unsteady parameter, and dimensionless nanoparticle volume friction; by increasing the magnitude of this parameter, resistance forces are produced which oppose the fluids particle motion, and due to this effect the skin friction increases. From Figures 8 and 9, we can see that the Nusselt number is the increasing function of the Eckert number, Prandtl number, and magnetic field parameter; physically, by enhancing the magnitude of these parameters the fluid particles motion is reduced, and, as a result, friction forces are produced, due to this Nusselt number

increasing. The convergence control parameter of the given problem was obtained up to the 25th iteration for both velocity and temperature distribution and presented in Tables 1 and 2. From Tables 1 and 2 we can see that as we increased the number of iterations, the residual error decreased, and a strong convergence was obtained on the approximate analytical solution. A comparison of the approximate analytical method to the numerical method is presented in Tables 3 and 4. Tables 5 and 6 represent the thermo-physical properties and thermo-conductivity of the nanofluids. The variation in magnetic field parameter  $M$  on the velocity profile is captured in Figure 1, for both MWCNT and SWCNT on  $f'(\eta)$ ; from Figure 1 we see that velocity is the decreasing function of the magnetic field parameter. Such a state happens due to the creation of a resistive force known as the Lorentz force. The magnitude of these forces increases with the increase of the magnetic field parameter, which oppose the fluid particle motion in the opposite direction; the motion of the fluid particles decreases, and as a result the velocity profile decreases. The variation in the dimensionless nanoparticle volume fraction parameter  $\phi$  on velocity profile is captured in Figure 2, for both the MWCNT and SWCNT velocity profile; from Figure 2 we can see that velocity is the decreasing function of the dimensionless nanoparticle volume fraction parameter  $\phi$ . Such a state happens due to the production of a resistive type force, known as viscose force. The strength of such a force increase with the increase in strength of the dimensionless nanoparticle volume fraction parameter  $\phi$ , which counteracts the motion of the fluid within the boundary layer and reduces the thickness of the boundary layer. The variation in the time-dependent parameter  $S$  in velocity profile is captured in Figure 3, and for both MWCNT and SWCNT we can see that velocity is the decreasing function of the time-dependent parameter  $S$ . Figure 4 shows the relation between Eckert number  $Ec$  and temperature profile; this relation is in direct relation, or the temperature profile is the increasing function of, Eckert number  $Ec$ . By increasing the Eckert number, this will improve the kinetic energy due to the intermolecular collision increasing, and, as a result, the temperature profile increases. Figure 5 shows the  $Pr$  for both MWCNT and SWCNT and the temperature distribution. It is noticeable from Figure 5 that the relation between  $\theta(\eta)$  and  $Pr$  is an inverse relation, where the largest value of  $Pr$  reduces the temperature distribution. Actually the thickness of the momentum boundary layer is superior than that of the thermal boundary layer, or the viscous diffusion is larger than the thermal diffusion, and, therefore, a larger Prandtl number reduces the thermal boundary layer; therefore, the Prandtl number was used as the Colling agent.

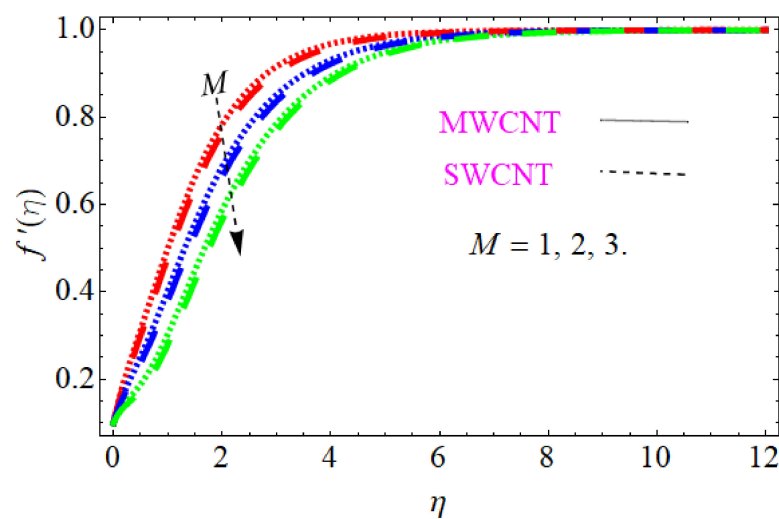


**Figure 1.** Consequence of  $M$  (magnetic field parameter) for velocity distribution.

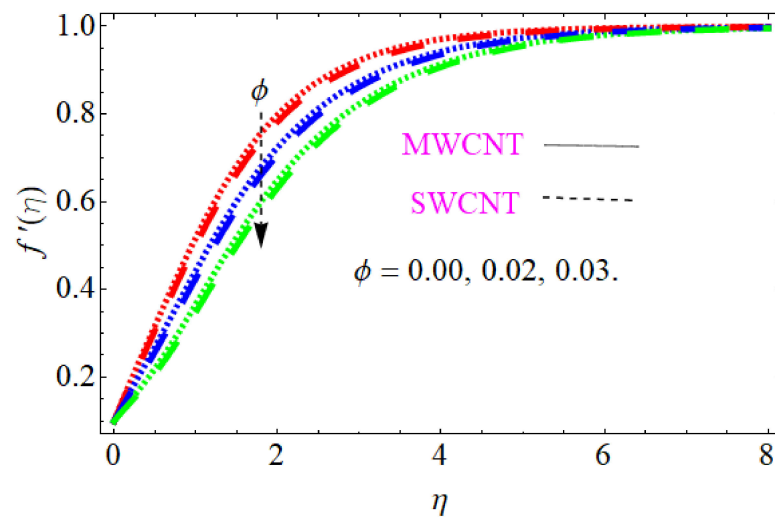


Figure 2. Consequence of dimensionless nanoparticle volume friction for velocity distribution.

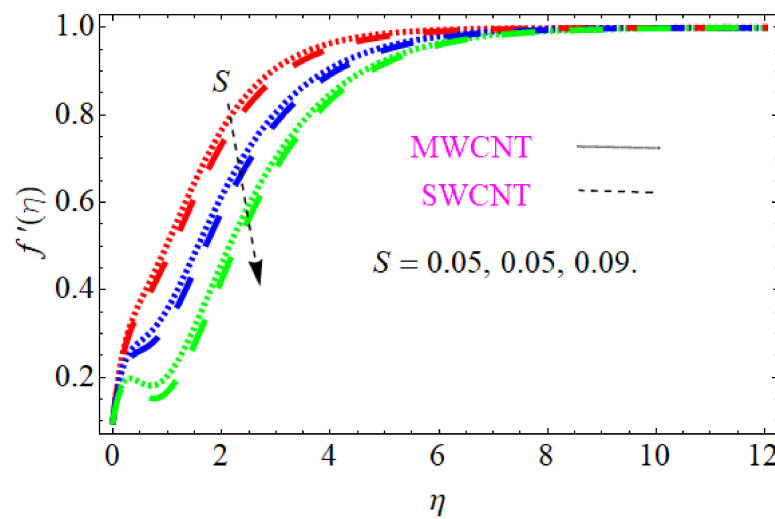


Figure 3. Consequence of unsteady parameter S for velocity distribution.

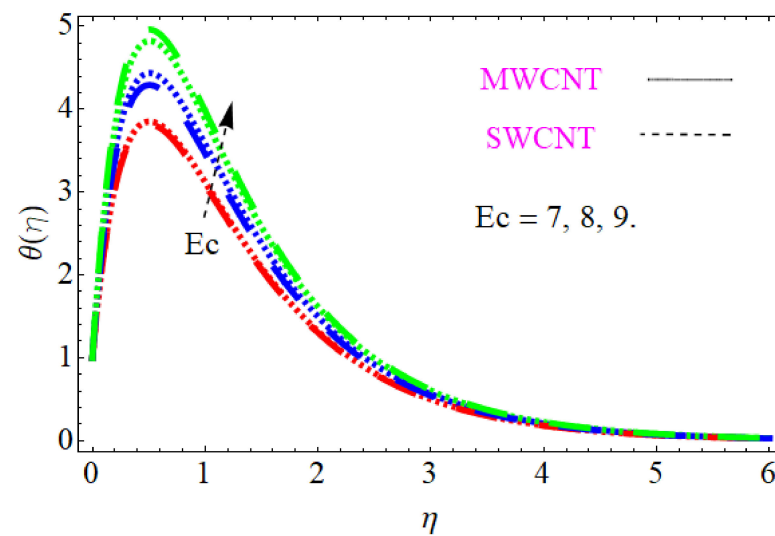


Figure 4. Consequence of the Eckert number for temperature distribution.

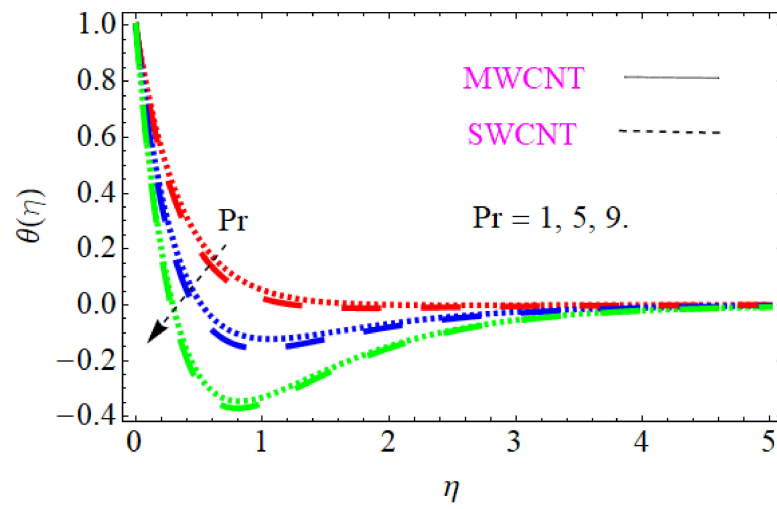


Figure 5. Consequence of Prandtl number for temperature distribution.

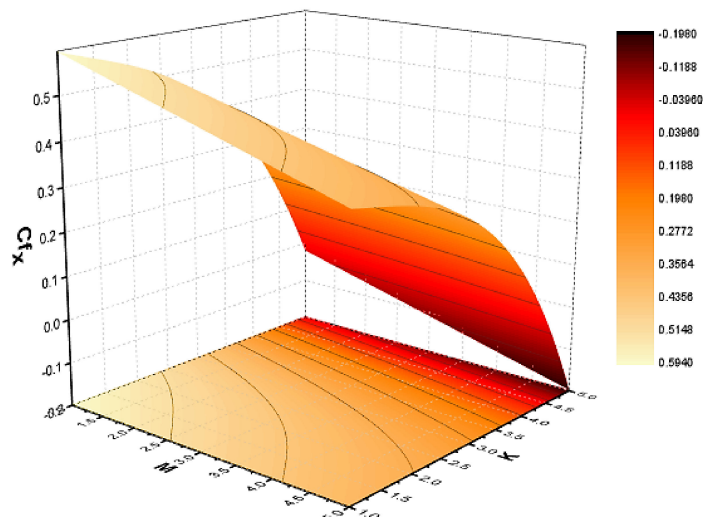


Figure 6. Effect of skin friction on M and S.

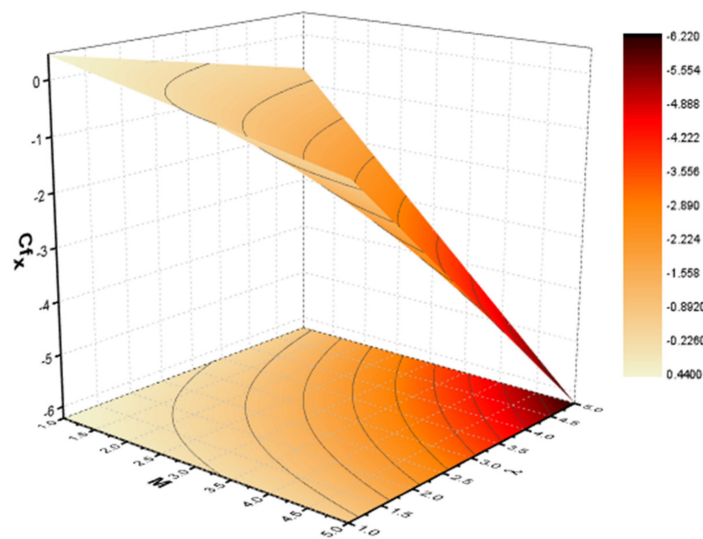


Figure 7. Effect on skin friction on M and  $\phi$ .



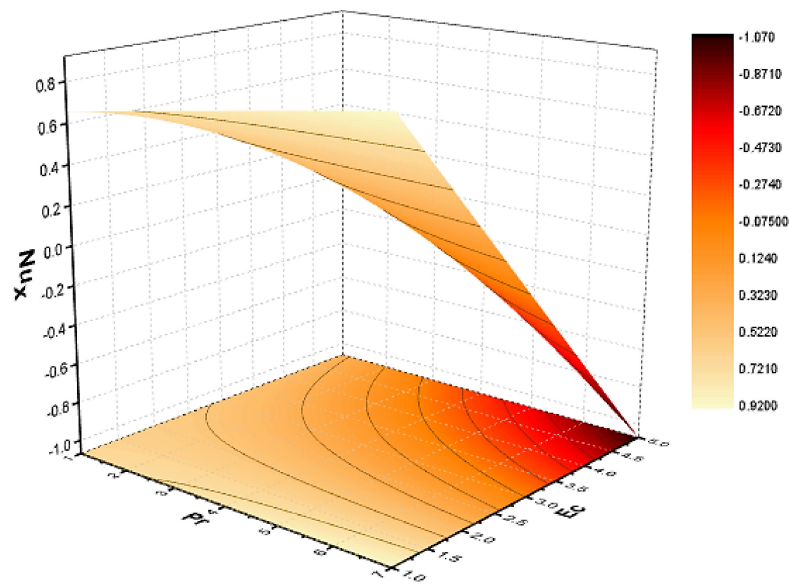


Figure 8. Effect of Nusselt number on Pr and Ec.

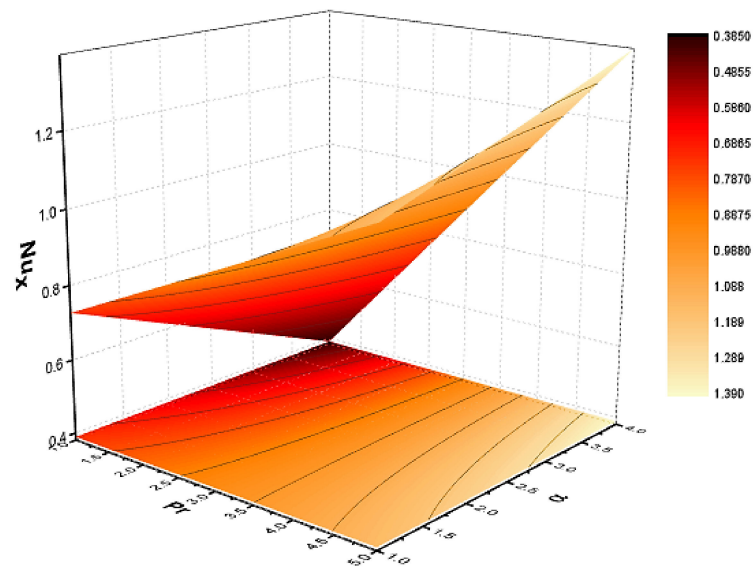


Figure 9. Effect of Nusselt number on Pr and M.

Table 1. Convergence of the method for MWCNT.

$m$	MWCNT	MWCNT
5	$0.1431 \times 10^{-1}$	$0.4775 \times 10^{-3}$
10	$0.3014 \times 10^{-2}$	$0.7873 \times 10^{-5}$
15	$0.3443 \times 10^{-3}$	$0.4729 \times 10^{-7}$
20	$0.9298 \times 10^{-5}$	$0.5453 \times 10^{-8}$
25	$0.3787 \times 10^{-7}$	$0.2412 \times 10^{-9}$

**Table 2.** Show the convergence of method for SWCNT.

$m$	SWCNT	SWCNT
5	$0.4391 \times 10^{-1}$	$0.4574 \times 10^{-1}$
10	$0.5166 \times 10^{-3}$	$0.7359 \times 10^{-2}$
15	$0.8238 \times 10^{-5}$	$0.7749 \times 10^{-5}$
20	$0.4626 \times 10^{-6}$	$0.3121 \times 10^{-7}$
25	$0.9433 \times 10^{-9}$	$0.5132 \times 10^{-9}$

**Table 3.** OHAM and numerical comparison for  $f(\eta)$ .

$m$	Numerical	OHAM	Absolute Error
1	1.00 . . . .	1.00 . . . .	0.0 . . . .
2	1.72 . . . .	1.70 . . . .	$2 \times 10^{-2}$ . . . .
3	1.71 . . . .	1.69 . . . .	$2 \times 10^{-2}$ . . . .
4	1.96 . . . .	1.94 . . . .	$2 \times 10^{-2}$ . . . .
5	0.87 . . . .	0.83 . . . .	$4 \times 10^{-2}$ . . . .
6	0.23 . . . .	0.21 . . . .	$2 \times 10^{-2}$ . . . .
7	0.29 . . . .	0.27 . . . .	$2 \times 10^{-2}$ . . . .
8	0.39 . . . .	0.38 . . . .	$1 \times 10^{-2}$ . . . .
9	0.42 . . . .	0.37 . . . .	$5 \times 10^{-2}$ . . . .
10	0.92 . . . .	0.90 . . . .	$2 \times 10^{-2}$ . . . .

**Table 4.** OHAM and numerical comparison for  $\theta(\eta)$ .

$\eta$	Numerical	OHAM	Absolute Error
1	1.00 . . . .	1.00 . . . .	0.0 . . . .
2	1.31 . . . .	1.29 . . . .	$2 \times 10^{-2}$ . . . .
3	1.12 . . . .	1.10 . . . .	$2 \times 10^{-2}$ . . . .
4	1.70 . . . .	1.65 . . . .	$5 \times 10^{-2}$ . . . .
5	1.44 . . . .	1.41 . . . .	$3 \times 10^{-2}$ . . . .
6	1.34 . . . .	1.30 . . . .	$4 \times 10^{-2}$ . . . .
7	1.95 . . . .	1.90 . . . .	$5 \times 10^{-2}$ . . . .
8	1.90 . . . .	1.80 . . . .	$1 \times 10^{-2}$ . . . .
9	1.54 . . . .	1.50 . . . .	$4 \times 10^{-2}$ . . . .
10	1.35 . . . .	1.30 . . . .	$5 \times 10^{-2}$ . . . .

**Table 5.** The thermo-physical properties.

Physical Properties		Thermal Conduct K(W/mk)	Specific Heat $C_p$ (J/kgK)	Density $\rho$ (kg/m <sup>3</sup> )
Solid particles	SWCNTs	6600	2600	2600
	MWCNTs	3000	1600	1600

**Table 6.** The thermal conductivity values at different volume fractions.

Volume Fraction $\phi$	0.0	0.01	0.02	0.03	0.04
$k_{nf}$ (SWCNTs)	0.145	0.147	0.204	0.235	0.266
$k_{nf}$ (MWCNTs)	0.145	0.172	0.2	0.228	0.2257

### 5. Conclusions

This paper examined the analytical investigation of the stagnation point flow of a CNT nanofluid over a stretching surface. In this research article, we used an approximate analytical method for the solution of the nonlinear differential equation to find a series solution for velocity and another for temperature profile. To transform the nonlinear partial differential equation (PDE) into a nonlinear ordinary differential equation (ODE), we

used the defined similarity transformation. By using the approximate analytical (OHAM) optimal homotopy asymptotic method to solve the obtained nonlinear ordinary differential equations. The impact of different parameters, such as magnetic field parameter, dimensionless nanoparticle volume fraction parameter, unsteady parameter, Prandtl number, and Eckert number were interpreted through graphs. The skin friction coefficient and Nusselt number were explained in the form of graphs. The present work was found to be in very good agreement with those published previously. The main outcomes of the present analysis are the following:

1. Increasing the value of the dimensionless nanoparticle volume fraction parameter reduces velocity.
2. Increasing the value of the magnetic field parameter reduces velocity
3. Increasing the value of the unsteady parameter reduces velocity
4. Increasing the value of the Prandtl number reduces the temperature profile
5. Increasing the value of the Eckert number increases the temperature profile

Of the numerous future physical world problems to be modeled in science and engineering, most of them will be nonlinear, so we cannot find the exact solution of the nonlinear differential equation for both the partial differential equation and ordinary differential equation; therefore, this method could be used in the future to find the approximate analytical series solution of the nonlinear differential equation, which has the best convergence to the exact solution. In the future, heat transfer phenomena will play a key role in engineering and industry. In our paper, we used a CNT nanofluid and discussed the heat transfer ratio, which plays an important role.

**Author Contributions:** Conceptualization, A.R.; methodology, A.R., A.S., Z.S., R.J. and P.K.; software, R.J.; validation, Z.S.; formal analysis, A.R. and A.S.; investigation, A.S. and R.J., resources, Z.S.; writing—original draft preparation, A.R.; writing—review and editing, A.S. and P.K.; visualization, Z.S. and R.J.; supervision, Z.S.; project administration, P.K.; funding acquisition, P.K. All authors have read and agreed to the published version of the manuscript.

**Funding:** The financial support provided by the Center of Excellence in Theoretical and Computational Science (TaCS-CoE), KMUTT. Moreover, this research project was supported by Thailand Science Research and Innovation (TSRI) Basic Research Fund: Fiscal year 2022 (FF65).

**Institutional Review Board Statement:** Not applicable.

**Informed Consent Statement:** Not applicable.

**Data Availability Statement:** All data used in this manuscript have been presented within the article.

**Acknowledgments:** The authors acknowledge the financial support provided by the Center of Excellence in Theoretical and Computational Science (TaCS-CoE), KMUTT. Moreover, this research project was supported by Thailand Science Research and Innovation (TSRI) Basic Research Fund: Fiscal year 2022 (FF65).

**Conflicts of Interest:** The authors have no conflict of interest.

## Nomenclature

$x, y$	Cartesian coordinates
$u, v$	Velocity components
$U_w, V_w$	Velocities of the stretching sheet
$S$	Time dependent parameter
$T$	Local Temperature
$M$	Magnetic field
$Nu_x$	Local Nusselt number
$pr$	Prandtl number
$T_w$	Surface temperature
$B_0$	Constant magnetic field

$T_{\infty}$	Ambient temperature-
$Ec$	Eckert number
$C_{fx}$	Skin friction coefficient in x– direction-
$\theta$	Dimensionless temperature
$\rho$	Density of the fluid
$\nu$	Fluid viscosity
$\eta$	Independent variable
$\lambda$	Spatial scale parameter
$k$	Thermal conductivity
$c_p$	Specific heat

## References

- Pop, I.; Postelnicu, A.; Grosan, T. Thermo-solutal Marangoni forced convection boundary layers. *Meccanica* **2001**, *36*, 555–571.
- Al-Mudhaf, A.; Chamkha, A.J. Similarity solutions for MHD thermo-solutal Marangoni convection over a flat surface in the presence of heat generation or absorption effects. *Heat Mass Transf.* **2005**, *42*, 112–121.
- Wang, C.Y. Liquid film sprayed on a stretching surface. *Chem. Eng. Commun.* **2006**, *193*, 869–878.
- Chen, C.-H. Marangoni effects on forced convection of power-law liquids in a thin film over a stretching surface. *Phys. Lett. A* **2007**, *370*, 51–57. [[CrossRef](#)]
- Magyari, E.; Chamkha, A.J. Exact analytical solutions for thermo-solutal Marangoni convection in the presence of heat and mass generation or consumption. *Heat Mass Transf.* **2007**, *43*, 965–974.
- Lin, Y.; Zheng, L.; Zhang, X. Magneto-hydrodynamics thermo-capillary Marangoni convection heat transfer of power-law fluids driven by temperature gradient. *J. Heat Transf.* **2013**, *135*, 051702.
- Lin, Y.; Zheng, L.; Zhang, X. Radiation effects on Marangoni convection flow and heat transfer in pseudo-plastic non-Newtonian nanofluids with variable thermal conductivity. *Int. J. Heat Mass Transf.* **2014**, *77*, 708–716. [[CrossRef](#)]
- Aly, E.; Ebaid, A. Exact analysis for the effect of heat transfer on MHD and radiation Marangoni boundary layer nanofluid flow past a surface embedded in a porous medium. *J. Mol. Liq.* **2016**, *215*, 625–639. [[CrossRef](#)]
- Ellahi, R.; Zeeshan, A.; Hassan, M. Particle shape effects on Marangoni convection boundary layer flow of a nanofluid. *Int. J. Numer. Methods Heat Fluid Flow* **2016**, *26*, 2160–2174. [[CrossRef](#)]
- Jiao, C.; Zheng, L.; Lin, Y.; Ma, L.; Chen, G. Marangoni abnormal convection heat transfer of power-law fluid driven by temperature gradient in porous medium with heat generation. *Int. J. Heat Mass Transf.* **2016**, *92*, 700–707. [[CrossRef](#)]
- Sheikholeslami, M.; Chamkha, A.J. Influence of Lorentz forces on nanofluid forced convection considering Marangoni convection. *J. Mol. Liq.* **2017**, *225*, 750–757. [[CrossRef](#)]
- Sheikholeslami, M.; Ganji, D.D. Influence of magnetic field on CuOeH<sub>2</sub>O nanofluid flow considering Marangoni boundary layer. *Int. J. Hydrog. Energy* **2017**, *42*, 2748–2755.
- Mahanthesh, B.; Gireesha, B.J.; PrasannaKumara, B.C.; Shashikumar, N.S. Marangoni convection radiative flow of dusty nanoliquid with exponential space dependent heat source. *Nucl. Eng. Technol.* **2017**, *49*, 1660–1668. [[CrossRef](#)]
- Sheikholeslami, M.; Ganji, D.D. Analytical investigation for Lorentz forces effect on nanofluid Marangoni boundary layer hydrothermal behavior using HAM. *Indian J. Phys.* **2017**, *91*, 1581–1587. [[CrossRef](#)]
- Mahanthesh, B.; Gireesha, B. Thermal Marangoni convection in two-phase flow of dusty Casson fluid. *Results Phys.* **2018**, *8*, 537–544. [[CrossRef](#)]
- Mahanthesh, B.; Gireesha, B.J. Scrutinization of thermal radiation, viscous dissipation and Joule heating effects on Marangoni convective two-phase flow of Casson fluid with fluid particle suspension. *Results Phys.* **2018**, *8*, 869–878.
- Choi, S.U.S. Enhancing thermal conductivity of fluids with nanoparticles. *ASME-Publ. Fed* **1995**, *231*, 99–106.
- Eastman, J.A.; Choi, S.U.S.; Li, S.; Yu, W.L.; Thompson, J. Anomalously increased effective thermal conductivities of ethylene glycol-based nano-fluids containing copper nanoparticles. *Appl. Phys.* **2001**, *78*, 718–720.
- Khamis, S.; Makinde, O.D.; Nkansah-Gyekye, Y. Unsteady flow of variable viscosity Cu-water and Al<sub>2</sub>O<sub>3</sub>-water nanofluids in a porous pipe with buoyancy force. *Int. J. Numer. Methods Heat Fluid Flow* **2015**, *25*, 1638–1657. [[CrossRef](#)]
- Malvandi, A.; Ganji, D.D. Mixed Convection of Alumina/Water Nanofluid in Microchannels using Modified Buongiorno's Model in Presence of Heat Source/Sink. *J. Appl. Fluid Mech.* **2016**, *9*, 2277–2289. [[CrossRef](#)]
- Reddy, S.; Chamkha, A.J. Heat and mass transfer characteristics of Al<sub>2</sub>O<sub>3</sub>-water and Ag-water nanofluid through porous media over a vertical cone with heat generation/absorption. *J. Porous Media* **2017**, *20*, 1–17. [[CrossRef](#)]
- Barnoon, P.; Toghraie, D. Numerical investigation of laminar flow and heat transfer of non-Newtonian nanofluid within a porous medium. *Powder Technol.* **2018**, *325*, 78–91. [[CrossRef](#)]
- Hosseini, S.; Sheikholeslami, M.; Ghasemian, M.; Ganji, D. Nanofluid heat transfer analysis in a microchannel heat sink (MCHS) under the effect of magnetic field by means of KKL model. *Powder Technol.* **2018**, *324*, 36–47. [[CrossRef](#)]
- Xie, H.; Lee, H.; Youn, W.; Choi, M. Nanofluids containing multiwalled carbon nanotubes and their enhanced thermal conductivities. *J. Appl. Phys.* **2003**, *94*, 4967. [[CrossRef](#)]
- Ding, Y.; Alias, H.; Wen, D.; Williams, R.A. Heat transfer of aqueous suspensions of carbon nanotubes (CNT nanofluids). *Int. J. Heat Mass Transf.* **2006**, *49*, 240–250. [[CrossRef](#)]

26. Haq, R.U.; Khan, Z.H.; Khan, W.A. Thermo-physical effects of carbon nanotubes on MHD flow over a stretching surface. *Phys. E Low-Dimens. Syst. Nanostruct.* **2014**, *63*, 215–222.
27. Ueki, Y.; Aoki, T.; Ueda, K.; Shibahara, M. Thermophysical properties of carbon-based material nanofluid. *Int. J. Heat Mass Transf.* **2017**, *113*, 1130–1134. [[CrossRef](#)]
28. Rehman, A.; Mehmood, R.; Nadeem, S.; Akbar, N.S.; Motsa, S.S. Effects of single and multi-walled carbon nanotubes on water and engine oil based rotating fluids with internal heating. *Adv. Powder Technol.* **2017**, *28*, 1991–2002.
29. Sreedevi, P.; Reddy, P.S.; Chamkha, A.J. Magneto-hydrodynamics heat and mass transfer analysis of single and multi-wall carbon nanotubes over vertical cone with convective boundary condition. *Int. J. Mech. Sci.* **2018**, *135*, 646–655. [[CrossRef](#)]
30. Jyothi, K.; Reddy, P.S.; Reddy, M.S. Influence of magnetic field and thermal radiation on convective flow of SWCNTs-water and MWCNTs-water nanofluid between rotating stretchable disks with convective boundary conditions. *Powder Technol.* **2018**, *331*, 326–337. [[CrossRef](#)]
31. Rahmati, A.; Reiszadeh, M. An experimental study on the effects of the use of multi-walled carbon nanotubes in ethylene glycol/water-based fluid with indirect heaters in gas pressure reducing stations. *Appl. Therm. Eng.* **2018**, *134*, 107–117. [[CrossRef](#)]
32. Muhammad, T.; Lu, D.-C.; Mahanthesh, B.; Eid, M.R.; Ramzan, M.; Dar, A. Significance of Darcy-Forchheimer Porous Medium in Nanofluid Through Carbon Nanotubes. *Commun. Theor. Phys.* **2018**, *70*, 361. [[CrossRef](#)]
33. Gau, H.; Herminghaus, S.; Lenz, P.; Lipowsky, R. Liquid morphologies on structured surfaces: From microchannels to microchips. *Science* **1999**, *283*, 46–49. [[PubMed](#)]
34. Binda, M.; Natali, D.; Iacchetti, A.; Sampietro, M. Integration of an organic photo-detector onto a plastic optical fiber by means of spray coating technique. *Adv. Mater.* **2013**, *25*, 4335–4339.
35. Kundan, A.; Nguyen, T.T.T.; Plawsky, J.L.; Wayner, J.P.C.; Chao, D.F.; Sicker, R.J. Condensation on Highly Superheated Surfaces: Unstable Thin Films in a Wickless Heat Pipe. *Phys. Rev. Lett.* **2017**, *118*, 094501. [[CrossRef](#)]
36. Frenkel, A.L. Nonlinear Theory of Strongly Undulating Thin Films Flowing Down Vertical Cylinders. *Eur. Lett.* **1992**, *18*, 583–588. [[CrossRef](#)]
37. Chang, H.-C.; Demekhin, E.A. Mechanism for drop formation on a coated vertical fibre. *J. Fluid Mech.* **1999**, *380*, 233–255. [[CrossRef](#)]
38. Kliakhandler, I.L.; Davis, S.H.; Bankoff, S.G. Viscous beads on vertical fibre. *J. Fluid Mech.* **2001**, *429*, 381–390. [[CrossRef](#)]
39. Duprat, C.; Giorgiutti-Dauphiné, F.; Tseluiko, D.; Saprykin, S.; Kalliadasis, S. Liquid film coating a fiber as a model system for the formation of bound states in active dispersive-dissipative nonlinear media. *Phys. Rev. Lett.* **2009**, *103*, 234501.
40. Ding, Z.; Wong, T.N. Three-dimensional dynamics of thin liquid films on vertical cylinders with Marangoni effect. *Phys. Fluids* **2017**, *29*, 011701. [[CrossRef](#)]
41. Alshomrani, A.S.; Gul, T. A convective study of Al<sub>2</sub>O<sub>3</sub>-H<sub>2</sub>O and Cu-H<sub>2</sub>O nano-liquid films sprayed over a stretching cylinder with viscous dissipation. *Eur. Phys. J. Plus* **2017**, *132*, 1–16.
42. AlSagari, A.S.; Nasir, S.; Gul, T.; Islam, S.; Nisar, K.; Shah, Z.; Khan, I. MHD Thin Film Flow and Thermal Analysis of Blood with CNTs Nanofluid. *Coatings* **2019**, *9*, 175. [[CrossRef](#)]
43. Chao, Y.; Ding, Z.; Liu, R. Dynamics of thin liquid films flowing down the non-isothermal cylinder with wall slippage. *Chem. Eng. Sci.* **2018**, *175*, 354–364.
44. Liao, S.-J. A kind of approximate solution technique which does not depend upon small parameters—II. An application in fluid mechanics. *Int. J. Non-Linear Mech.* **1997**, *32*, 815–822. [[CrossRef](#)]
45. Liao, S. On the homotopy analysis method for nonlinear problems. *Appl. Math. Comput.* **2004**, *147*, 499–513. [[CrossRef](#)]
46. Liao, S.J. *Homotopy Analysis Method in Non-Linear Differential Equations*; Springer: Berlin/Heidelberg, Germany, 2012.
47. Gul, T.; Ferdous, K. The experimental study to examine the stable dispersion of the graphene nanoparticles and to look at the GO-H<sub>2</sub>O nanofluid flow between two rotating disks. *Appl. Nanosci.* **2018**, *8*, 1711–1728.
48. Gul, T.; Nasir, S.; Islam, S.; Shah, Z.; Khan, M.A. Effective Prandtl Number Model Influences on the  $\gamma$ -Al<sub>2</sub>O<sub>3</sub>-AH<sub>2</sub>O and  $\gamma$ -Al<sub>2</sub>O<sub>3</sub>-C<sub>2</sub>H<sub>6</sub>O<sub>2</sub> Nanofluids Spray Along a Stretching Cylinder. *Arab. J. Sci. Eng.* **2018**, *44*, 1–16.
49. Gohar, T.; Gul, W.; Khan, M.; Shuaib, M.; Khan, M.; Bonyah, E. MWCNTs/SWCNTs Nanofluid Thin Film Flow over a Non-linear Extending Disc: OHAM Solution. *J. Therm. Sci.* **2019**, *28*, 115–122.
50. Gul, T.; Haleem, I.; Ullah, I.; Khan, M.A.; Bonyah, E.; Khan, I.; Shuaib, M. The study of the entropy generation in a thin film flow with variable fluid properties past over a stretching sheet. *Adv. Mech. Eng.* **2018**, *10*, 1687814018789522. [[CrossRef](#)]
51. Khan, W.; Idress, M.; Gul, T.; Khan, A.M.; Bonyah, E. Three non-Newtonian fluids flow considering thin film over an un-steady stretching surface with variable fluid properties. *Adv. Mech. Eng.* **2018**, *10*, 1687814018807361.